THE JOURNAL OF PHYSICAL CHEMISTRY B

Article

pubs.acs.org/JPCB

Are Micelles Needed to Form Methane Hydrates in Sodium Dodecyl Sulfate Solutions?

M. Albertí,*[,†] A. Costantini,[‡] A. Laganá,[‡] and F. Pirani[‡]

[†]IQTCUB, Departament de Química Física, Universitat de Barcelona, Barcelona, Spain

[‡]Dipartimento di Chimica, Università di Perugia, Perugia, Italy

ABSTRACT: The possibility that methane hydrates form in sodium dodecyl sulfate (SDS) water solutions without the help of micelles formation has been investigated. To asses whether micelles are needed for the hydrate to form only one SDS molecule has been considered. To figure out the possible mechanism through which the SDS promotes the formation of methane clathrate the dynamics of CH_4 solvation in the presence and absence of the surfactant molecule is monitored. To carry out the dynamical calculations, the SDS-H_2O, SDS-CH_4, and CH_4-H_2O interactions were described using a recently proposed model potential. The adopted model leverages both on the decomposition of the molecular polarizability in effective components associated with the interaction centers distributed on the molecular frame and on the use of an improved Lennard-Jones functional form to represent the effective pair interaction energies. Molecular dynamics simulations performed on such potential, contrary to some earlier assumptions, do not support mechanisms requiring the formation of micelles as suggested by the findings of more recent experiments.

Incipient formation of a clathrate structure

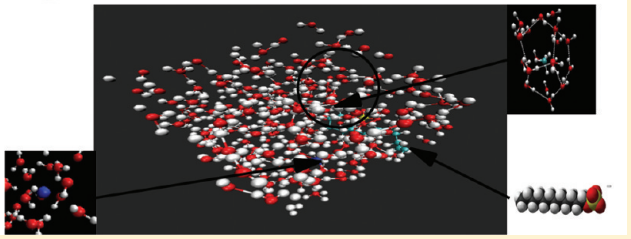

1. INTRODUCTION

Gas hydrates are icelike solid inclusion compounds which result from the trapping of gas molecules within a latticelike cage of water molecules. Many gases have molecular sizes suited to form hydrates like methane (CH_4) and carbon dioxide (CO_2). Gas hydrates are, in fact, essentially water clathrates in which the water cage crystallizes in the isometric crystallographic system rather than in the hexagonal one of normal ice.[1] Actually, the cage of water molecules (host) is stabilized by the trapped gas molecule (guest), and without such contribution, the lattice structure of hydrate clathrates would collapse into a conventional ice crystal structure or liquid water.

Clathrates became famous some time ago because of their ability to obstruct natural gas pipelines.[2] Light gases, such as methane or ethane, always present in oil products, at low temperature and high pressure, can get trapped as guest molecules in hydrate structures and make them solidify.[3] However, important benefits can be derived from the exploitation of this property. For instance, at standard conditions of pressure and temperature, one volume of methane hydrate can store up to 164 volumes of gaseous methane,[3] allowing its safer and cheaper storage and transportation. Because of this methane hydrates can be considered the most abundant carbon-based energy source on Earth[4,5] (conservatively estimated to amount to about twice the quantity of carbon in all known fossil fuels), and this makes the sedimentary methane hydrate reservoirs a potentially important source of hydrocarbon fuels. Moreover, the lower stability of the CH_4 clathrate with respect to that of CO_2 has suggested the use of extraction of methane from clathrates together with the adoption of carbon dioxide mitigation techniques based on the sequestering of CO_2 in hydrates.[6,7]

The mechanisms of formation of a gas hydrate involves typically the following steps: gas dissolution, formation of crystallographic nuclei, and their growth. The bottleneck for such mechanism is the formation of the solvent cage that needs long induction time and has a low rate.[8] On the theoretical side, the determination of the steps of such mechanism and of the structure of the water cages formed by the host molecules (determined by non covalent forces,[6,9]) prompts an accurate description of the interaction and a rationalization of the aggregation forms of the solvent in the presence of the guest gas. On its side the experiment has already indicated that the formation of the solvent cage depends on the interfacial area, pressure, temperature as well as on the extent of supercooling.[10] The experiment has also singled out that, after a certain induction time, the structure of gas hydrates grows mainly at the gas−water interface[11] with the rate of formation of the clathrate being controlled by the gas diffusion rate through the hydrate film.

The gas diffusion is enhanced by some additives, like the surfactants (*surface active agents*), whose molecules have lipophilic and hydrophilic moieties (amphiphilic molecules). This property has been rationalized in terms of a reduction of the surface tension at gas−water interface by the surfactant that facilitates the gas diffusion into water.[12] To this end, Zhang et

Received: February 3, 2012
Revised: March 20, 2012
Published: March 26, 2012

al.,[13] when investigating the behavior of sodium dodecyl sulfate (SDS) solutions, suggested that SDS molecules adsorb on hydrate nuclei and reduce the energy barrier for further aggregation. This was rationalized, at least in a certain concentration range, in terms of a tendency of the surfactant molecules to form micelles which can act as effective sites for hydrate nucleation.[14] Yet, a few years later, thanks to the analysis of the critical micelle concentration (CMC) of several surfactants, it was demonstrated[15] that no micelles intervene during the formation of the gas hydrate.

To put that finding on a robust theoretical ground we started extended calculations aimed at modeling the mechanism of formation of gas hydrates when surfactants are added to the water−gas system.[16−19] To this end, a recently developed model potential,[20−27] based on the decomposition of the molecular polarizability into effective components and using a new formulation of noncovalent interactions, has been utilized to build an appropriate potential energy surface (PES). Such PES has been used to carry out molecular dynamics (MD) simulations for systems containing SDS-CH_4, SDS-H_2O, CH_4-H_2O, and SDS-CH_4-H_2O by running the DL-POLY[28] package. The package was implemented on a local cluster of the IQTCUB at the University of Barcelona and on the EGI Grid Infrastructure available to the virtual organization (VO) COMPCHEM[29] (COMPCHEM is a community of molecular and material scientists committed to foster grid calculations and to enhance the assemblage of the so-called grid-empowered molecular simulator GEMS[30]).

The present study concerns the investigation of a system made of only one molecule of SDS and one of CH_4 in an environment of 2000 water molecules. In spite of the fact that such molecular composition corresponds to a concentration of SDS in water larger than the critical micelle concentration, the consideration of only one molecule of SDS ensures the absence of micelles. Accordingly, the possible formation of ordered clathrate type structures can be attributed to the capability of SDS to organize water molecules in such a way that methane is driven and then dropped inside the cage. Accordingly, the paper is articulated as follows: in section 2 the potential energy function is illustrated. In sections 3 and 4, the formation of solvation spheres and the formation of the gas hydrate itself are discussed.

2. POTENTIAL ENERGY SURFACE

As usual in our studies,[26,27,31,32] the PES of the investigated system is formulated as a sum of intermolecular (V_{inter}) and intramolecular (V_{intra}) contributions. The first ones determine the structure of the aggregates, and the second ones affect the conformations assumed by the SDS molecule under various conditions (see below). V_{inter} is further decomposed into non electrostatic (V_{nelec}) and electrostatic (V_{elec}) terms, which are assumed to be independent. V_{nelec} depends on the balancing of van der Waals components associated with the various centers distributed on the molecular frame. Therefore it is usually expressed in terms of the corresponding pair interactions between individual atoms (or groups of atoms), having a given effective polarizability. Yet, both water and methane have small molecular polarizability compared with that of SDS. Accordingly, no decomposition was attempted for them, and single interaction centers, placed on the O and on the C atoms (marked as Ow and Cm) of H_2O and CH_4, respectively, were considered (the successful use of a single interaction center has been already documented in the past for H_2O[33−39] and CH_4[19]).

For the molecular polarizability of the SDS molecule (CH_3-$(CH_2)_{11}$-SO_4Na), instead, a decomposition in effective polarizability values associated with the CH_3-, CH_2-, $(-SO_4)^-$, and Na^+ groups (whose interaction centers are labeled as C3, C2, SO, and Na and assumed to be placed on the C, S, and Na atoms, respectively) was made. This decomposition was applied to the description of both V_{intra} and V_{inter} for SDS-CH_4. On the contrary, the effective polarizability associated with the individual atoms of the $(-SO_4)^-$ group were considered for the description of the SDS-H_2O interaction to the end of avoiding the collapse caused by the electrostatic attraction acting between point charges distributed on both molecular frames. Pair interactions acting between centers having an effective polarizability and describing the base (V_{nelec}) components of V_{inter} and V_{intra} (see below) are formulated in terms of an Improved Lennard-Jones (ILJ) function[36,40] as follows

$$V_{ILJ} = \varepsilon\left[c_1\left(\frac{r_0}{r}\right)^{\beta+4.0\left(\frac{r}{r_0}\right)^2} - c_2\left(\frac{r_0}{r}\right)^m\right] \quad (1)$$

with

$$c_1 = \frac{m}{\beta + 4.0\left(\frac{r}{r_0}\right)^2 - m} \quad (2)$$

$$c_2 = \frac{\beta + 4.0\left(\frac{r}{r_0}\right)^2}{\beta + 4.0\left(\frac{r}{r_0}\right)^2 - m} \quad (3)$$

Equation 1 contains four parameters; two of which, ε and r_0 (also used in the traditional Lennard-Jones (LJ) function), are the well depth and the equilibrium distance (i.e., the point at $V_{ILJ} = -\varepsilon$) of each interaction pair, respectively. They have a specific physical meaning and are transferable among different systems[25,36,38,39] ensuring that all partners are equally well described at both intramolecular and intermolecular level. The third parameter, β, defining the falloff of the repulsion and the relative strength of repulsion and attraction, depends on the nature of the environment, and therefore, is only partially transferable. The fourth parameter, m, depends on the nature of the attraction, and as usual, $m = 6$ was chosen in the case of a dominant dispersion attraction contribution (when the ion-induced dipole attraction dominates the dispersion one m is taken equal to 4).

The values of the parameters, obtained from the effective polarizability for the considered groups[41] are given in Table 1. The Ow-Ow parameters and the associated electrostatic contributions used in the present study are those previously tested in the modeling of liquid water (made of non rigid H_2O molecules),[36] while the Ow-Na^+ ones are the same as those already used in the study of the water solvation of M^+ ions (M = Na, K, Rb)[42] and of M^+-Benzene dimers.[34]

In the methane molecule C and H atoms, because of their shared electron pairs, have similar electronegativity. Moreover, the high symmetry of CH_4 and the absence of permanent dipole and quadrupole moments prompts the use of a null effective charge on each atom.[44] Accordingly, the electrostatic energy V_{elec} is calculated only from the charge distribution of the SDS and water molecules. The monomer geometry and the charge distribution of water are the ones used before to

dx.doi.org/10.1021/jp301124z | J. Phys. Chem. B 2012, 116, 4220−4227

Table 1. Values of ε (Well Depth), r_0 (Equilibrium Distance), β, and m Parameters Used to Define the Pair Interactions in Eqs 1 and 2[a]

interaction partners	ε/meV	r_0/Å	β	m
C2-C2	10.86	3.886	8	6
C2-C3	11.70	3.919	8	6
C2-SO	20.69	4.422	8	6
C3-SO	22.91	4.440	8	6
C3-Ow	10.56	3.850	8	6
C2-Ow	9.85	3.814	8	6
S-Ow	6.96	3.946	8	6
O-Ow	6.96	3.946	8	6
C3-Na^+	2.86	3.595	8	6
C2-Na^+	2.76	3.538	8	6
S-Na^+	1.75	3.742	8	6
O-Na^+	1.75	3.742	8	6
Ow-Na^+	151.89	2.732	6.5	4
Ow-Ow	9.06	3.730	7.5	6
Cm-Na^+	2.91	3.676	8	6
Cm-C3	13.73	3.999	8	6
Cm-C2	12.67	3.968	8	6
Cm-SO	25.75	4.467	8	6
Cm-Ow	13.18	3.868	8	6
Cm-Cm	14.98	4.040	8	6

[a]In some cases data do not include the effect of the long-range induction attraction, strongly attenuated by nonadditive many-body effects[43] (Cm−Na^+ and Cm−SO) or dominated by the electrostatic components (Ow−O).

investigate flexible molecules[36] and correspond to a dipole moment equal to 2.4 D. For SDS the same charge distribution adopted for the MD simulations of micelles formation in water,[45] is used.

Then, the CH_4-H_2O interaction ($V_{CH_4\text{-}H_2O}$) is formulated using a single pair interaction between the two effective centers Ow and Cm. The reliability of the interaction has been analyzed by comparing model predictions with accurate ab initio calculations.[46] Such comparison shows that our effective radial potential exhibits both repulsive and attractive components falling, at all intermolecular distances, within the ranges of energy calculated for various configurations of the system. Moreover, the same radial term provides values of the second virial coefficient in reasonable agreement with experimental data, especially at high temperature where anisotropy effects tend to vanish.

The SDS-CH_4 interaction ($V_{SDS\text{-}CH_4}$) is formulated as

$$V_{SDS-CH_4} = V_{CH_4-CH_3} + \sum_{i=1}^{11} V_{CH_4-(CH_2)_i} + V_{CH_4-SO_4} + V_{CH_4-Na} \quad (4)$$

On the contrary, the SDS-H_2O interaction is formulated using a different decomposition of the molecular polarizability and including the strong electrostatic effects as follows

$$V_{SDS-H_2O} = V_{H_2O-CH_3} + \sum_{i=1}^{11} V_{H_2O-(CH_2)_i} + \sum_{i=1}^{4} V_{H_2O-(O)_i} + V_{H_2O-S} + V_{H_2O-Na} + V_{elec} \quad (5)$$

where V_{elec} is calculated from the previously mentioned charge distributions of SDS and water.

As to V_{intra}, that of the H_2O molecule is taken from ref 36, while that of the SDS molecule, is formulated as a sum of the covalent bond (V_{bnd}), the angle (V_{ang}), and the dihedral (V_{dih}) interaction terms plus the noncovalent V_{nelec} contributions. For the V_{bnd} and V_{ang} description the parameters are taken from the

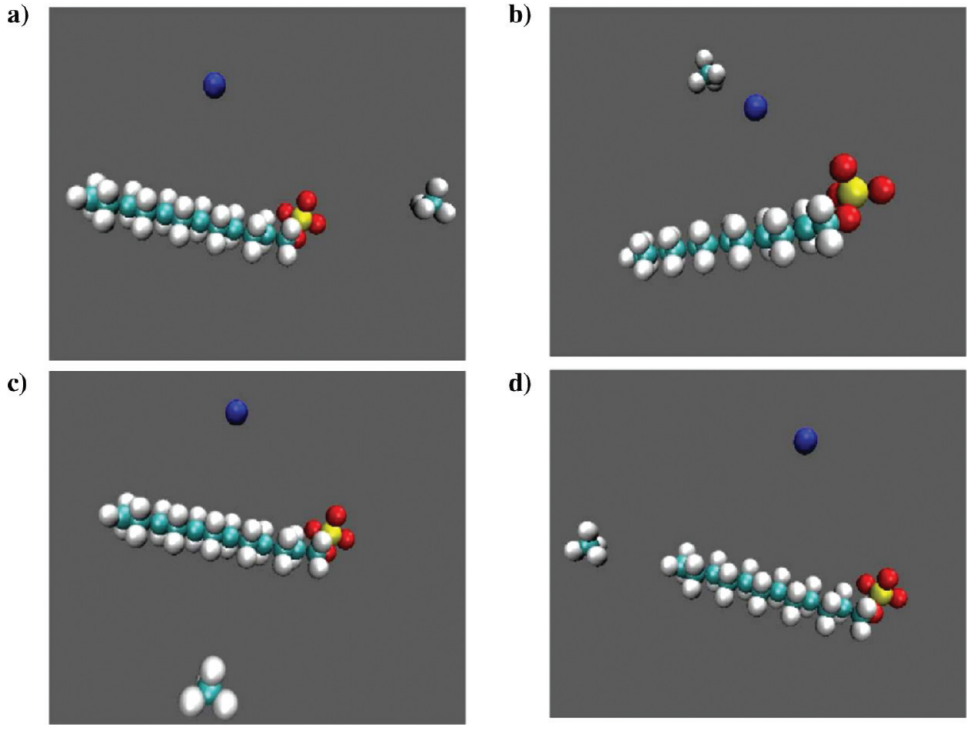

Figure 1. The four different initial configurations of the SDS-CH_4 system considered.

dx.doi.org/10.1021/jp301124z | J. Phys. Chem. B 2012, 116, 4220−4227

AMBER Intramolecular Generalized Force Field,[47] while for V_{dih} those of ref 45 are adopted. The remaining noncovalent contributions are calculated by adopting the above-mentioned ILJ function and the same decomposition of the SDS polarizability used to describe the SDS-CH_4 intermolecular interaction. The pairs considered are CH_3-CH_2, CH_2-CH_2, CH_3-SO_4, CH_2-SO_4, CH_3-Na, CH_2-Na, and SO_4-Na whose values for the related ILJ function parameters are given in Table 1.

3. FROM DIMERS TO SOLVATION SPHERES SIMULATIONS

To analyze the validity and the effectiveness of the proposed interaction we carried out, first, MD simulations for the separate SDS-CH_4, SDS-H_2O, and CH_4-H_2O systems using the DL-POLY program.[28] Following the same procedure of previous works[38,39] (which involves the evaluation of the interaction energy associated with various geometries of the dimer and the extrapolation of the results at low temperature (0 K)), the equilibrium-like structures for both the SDS-CH_4 and SDS-H_2O systems were determined first. Then the obtained equilibrium-like structure of SDS-CH_4 was solvated by merely surrounding such aggregate by water molecules, and from this the MD simulations of the SDS-CH_4-$(H_2O)_n$ system were started. In this way the calculations are not biased to the formation of clathrate cages and the comparison of the outcomes of the CH_4-$(H_2O)_n$ and the SDS-CH_4-$(H_2O)n$ MD calculations can single out the role played by SDS in promoting the formation of methane hydrates.

The equilibrium-like structures for both SDS-H_2O and SDS-CH_4 have been determined from the angular distribution functions obtained at low temperatures considering a micro-canonical ensemble of particles (NVE).[19] A time step of 1 fs and a cutoff radius of 9 Å were adopted to keep the variation of the total energy (E_{total}) smaller than 10^{-5} meV for all the simulations. After equilibration, during which the system tends to reach one of the most stable configurations, the MD trajectories for SDS-H_2O and SDS-CH_4 were integrated by conserving E_{total} to allow a statistical analysis.

The MD simulations of the SDS-CH_4 dimer were started from the four limiting initial configurations shown in Figure 1. All the low-temperature calculations (at low temperature the mean configuration energy (E_{cfg}) is close to the equilibrium one) led, after 0.1 ns of equilibration and an additional 1 ns of simulation, to a configuration having the sulfate head closely located near the methane molecule (see Figure 2). Such configuration is easily reached during the equilibration period and becomes, therefore, the geometry of election for starting subsequent simulations. The system, in fact, once equilibrated at the desired temperature, can explore for a sufficient long time those regions of the phase space compatible with the corresponding value of E_{total} (and therefore of T).

As a matter of fact, by carrying out a low-temperature analysis of the distributions of the associated distances and angles, it was possible to locate the geometries at which the potential energy has a minimum (for the sake of clarity we state again here that we take as equilibrium-like geometry that of T = 5 K, the lowest studied temperature). Strictly speaking, in fact, the characteristics of the global minima should be determined by means of a global optimization studies.[48,49] However, the fact that very similar final structures are obtained starting from various configurations and different values of T supports the idea that final structures are very close to the equilibrium one.

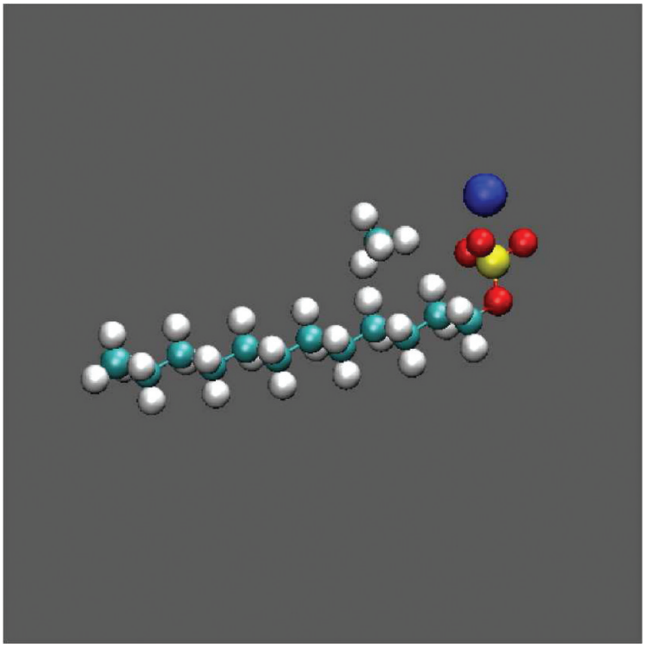

Figure 2. SDS-CH_4 equilibrium-like structure obtained at T = 5 K.

Thus, the distributions of the distances and of the angle values obtained from the simulation should largely coincide with those associated with the preferred geometry of the dimer (see Figure 3 in which the upper panel shows the radial distribution

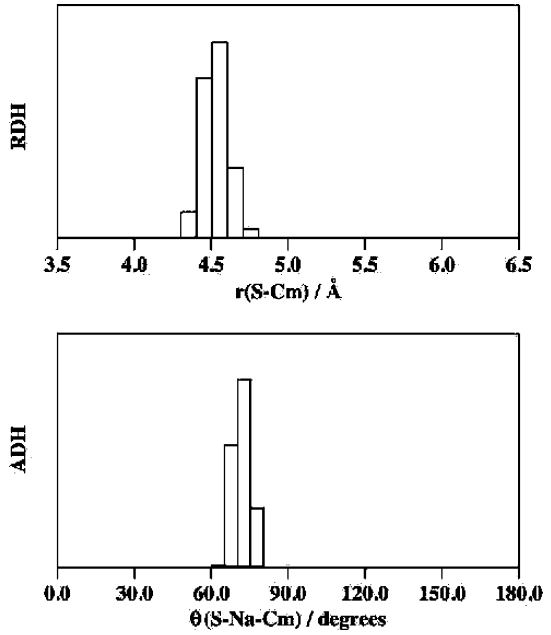

Figure 3. S-Cm RDH (top panel) and S-Na-Cm ADH (bottom panel) obtained at T = 5 K.

histogram (RDH) of methane with respect to the S atom while the lower panel shows the corresponding S-Na-CH_4 angular distribution histogram (ADH)). The two histograms indicate that the distribution of the S-CH_4 distance values peaks at about 4.63 Å and that of the S-Na-CH_4 angles peaks around of 71.14°.

The result of the similar investigation performed for the SDS-H_2O dimer (using again a NVE statistical ensemble of

dx.doi.org/10.1021/jp301124z | J. Phys. Chem. B 2012, 116, 4220−4227

atoms) are shown in Figure 4 (upper panel, the RDH of water with respect to the S atom; lower panel, the corresponding

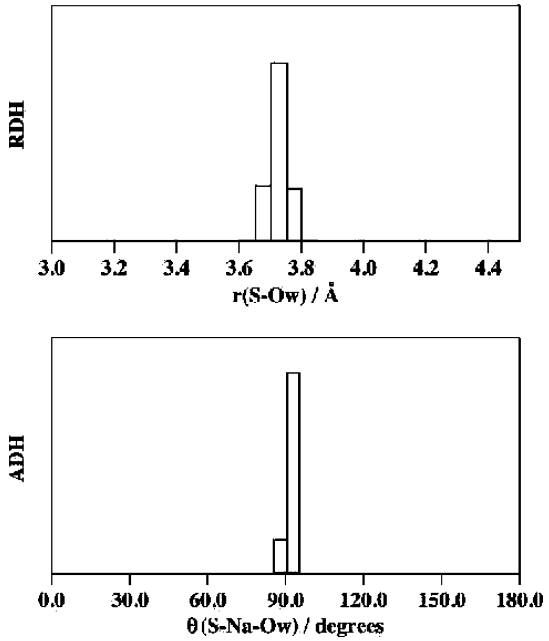

Figure 4. S-Ow RDH (top panel) and S-Na-Ow ADH (bottom panel) obtained at T = 5 K.

ADH for S-Na-H_2O). The calculations suggest that the Ow atom of the water molecule is preferentially located about 3.76 Å far from the S atom and forms an angle of 92.70° with Na^+.

Additional simulations were performed for both the SDS-$(H_2O)_n$ and the CH_4-$(H_2O)_n$ systems for an increasing number n of nonordered configurations of water molecules. For them, the same conditions adopted for the previous NVE simulations were employed and the radial distribution functions (RDF)[50] were evaluated to the end of determining the preferred radius of the first solvation shell (ISr).

The configuration energy per water molecule ($E_{cfg}/n(H_2O)$) and the ISr, derived in this way are reported in Tables 2 and 3 for the CH_4-$(H_2O)_n$ and the SDS-$(H_2O)_n$ systems, respectively, for increasing values of n.

Table 2. $E_{cfg}/n(H_2O)$ and First Solvation Shell Preferred Radius for Different Numbers of Water Molecules Solvating CH_4 (CH_4-$(H_2O)_n$ System)

n	$E_{cfg}/n(H_2O)$ (eV)	ISr (Å)
32	−0.4683	4.05
69	−0.4706	3.88
168	−0.4645	3.78

Table 3. $E_{cfg}/n(H_2O)$ and First Solvation Shell Preferred Radius for Different Numbers of Water Molecules Solvating SDS (SDS-$(H_2O)_n$ System)

n	$E_{cfg}/n(H_2O)$ (eV)	ISr (Å)
30	−0.7531	3.86
63	−0.6156	3.56
170	−0.4749	4.03

As the minimum cavity structure able to encapsulate a methane molecule is the 5^{12} one (defined as a pentagonal dodecahedron cage) formed by 20 molecules of water, a minimum of 60 molecules are required to carry out the analysis of the formation of a crystal of methane hydrate (cubic I). Accordingly, the comparison of the properties of water ensembles containing less than 60 molecules for CH_4-$(H_2O)_n$ with those of the ensembles containing more than 60 molecules gives information about the ability of methane to form structured hydrates as the number of water molecules increases. MD results for the CH_4-$(H_2O)_n$ system do not show any tendency to form ordered geometries when the number of water molecules increases, even if for larger numbers of water molecules the first peak of the radial distribution function shifts to lower distances. As a matter of fact, for the CH_4-$(H_2O)_n$ system it has been observed (see Table 2) that the value of $E_{cfg}/n(H_2O)$ is almost independent of n. On the contrary, as shown in Table 3, an increase of the number of water molecules for the SDS-$(H_2O)_n$ system leads to an increase (less negative value) for $E_{cfg}/n(H_2O)$, in agreement with the results of ref 51 for SDS-water bulk.

To complete the picture, the characteristics of the SDS-CH_4-$(H_2O)_n$ system have been also investigated by considering ensembles of 64 and 168 water molecules. As apparent from the results given in Table 4, in which the $E_{cfg}/n(H_2O)$ and ISr

Table 4. $E_{cfg}/n(H_2O)$ and First Solvation Shell Preferred Radius for Different Numbers of Water Molecules Solvating CH_4 (SDS-CH_4-$(H_2O)_n$ System)

n	$E_{cfg}/n(H_2O)$ (eV)	ISr (Å)
64	−0.6011	3.56
168	−0.5564	3.78

(referred to the preferred distances between the O atom of water and the C atom of methane) are given, an increase of the number of water molecules surrounding the SDS-CH_4 dimer leads to an increase of the configuration energy of the system and, at the same time, to an increase of the size of the first solvation shell of CH_4. Therefore, by comparing the results of Table 2 and Table 4, it can be concluded that the position of the first solvation peak does not depend on the presence of the SDS molecule when the number of water molecules becomes large.

4. THE CLATHRATE FORMATION SIMULATION

The next step of the investigation focused on an analogous MD simulation for a solvated SDS-CH_4 dimer under conditions of temperature and pressure typical of clathrate formation, to single out the role played in the process by the SDS molecule. Such simulations were performed by considering a NpT ensemble of particles (adopting for it cubic boundary conditions) using the same time step and cutoff as in the previously mentioned NVE calculations. As initial configuration we took the already discussed equilibrium-like geometry of SDS-CH_4, immersed into an ensemble of 2000 nonrigid[36] nonordered water molecules (SDS-$CH_4(H_2O)_{2000}$), as illustrated in Figure 5, so as not to favor, as mentioned before, any initially solvated CH_4 structures. A volume of 40 $Å^3$ was chosen and the possibility of hydrate formation has been investigated under different conditions of temperature and pressure. To integrate MD trajectories a time step of 1 fs and an

dx.doi.org/10.1021/jp301124z | J. Phys. Chem. B 2012, 116, 4220−4227

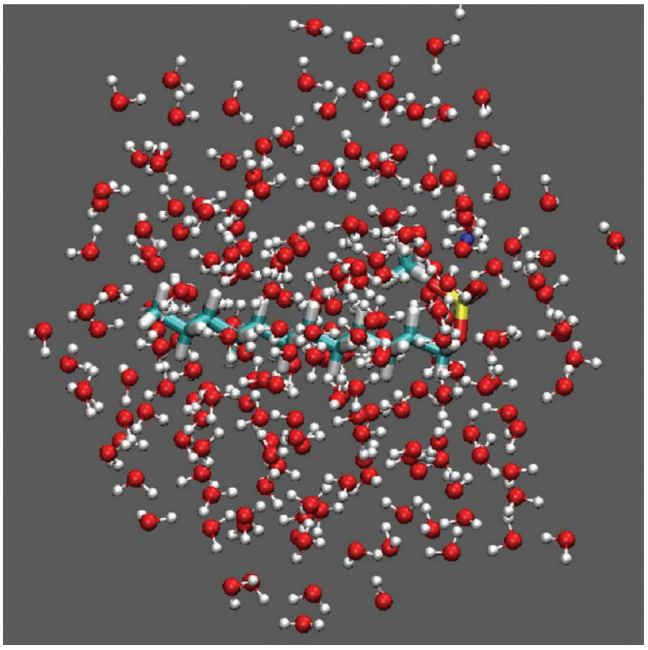

Figure 5. Sketch of the SDS-CH_4 equilibrium-like structure, obtained at T = 5 K, surrounded by an ensemble of 170 randomly oriented water molecules.

equilibration time of 40 ps were used in all the simulations. The MD trajectories were integrated for an overall time of 2 ns.

As indicated by Koh et al.,[52] the hydration sphere around methane in the liquid changes dramatically when forming the hydrate. It is, therefore, difficult to carry out a MD simulation of the formation of clathrate hydrates by starting from disordered initial structures. However, when Koh et al. analyzed water ordering during hydrate formation, they found that at the onset of the process only slight changes in the methane-water coordination had occurred. It seems, in fact, that once the hydrate starts to form, the hydration shell becomes, on average, slightly less ordered than in the methane solution. In spite of these difficulties, we have investigated RDFs in order to test the capability of the potential energy function to describe the selective role of clathrate hydrate interactions. The temperature dependence has been evaluated in two runs at 275 and 291 K, and the pressure influence has been evaluated in two runs performed at 8 and 14.5 MPa. With T = 275 K and p = 8 MPa a condition in which the natural hydrates are stable, and T = 292 K at p = 14.5 MPa, a temperature value 5 K above the methane hydrate melting line,[53] these p and T conditions seems to be suitable values to investigate the occurrence of possible structural changes of methane hydrate.

As it has been indicated before, the initial configuration considered to investigate the behavior of SDS-CH_4-$(H_2O)_{2000}$ system is that of the equilibrium for the SDS-CH_4 dimer. Accordingly, the initial distance from the sulfur atom (S) of SDS and the carbon atom of CH_4 (Cm) is about a value of 4.5 Å (see Figure 3). MD simulations show an increase of the S-Cm distance, indicating that in presence of water; SDS little interacts with CH_4 for a long time. This finding can be quantified by considering the S-Cm radial distribution function, which does not show any specific order, while suggesting a propensity of CH_4 to stay large distances far from S (see Figure 6). Similar results are obtained using different conditions of T and p. This seems to indicate that SDS and CH_4 preferably

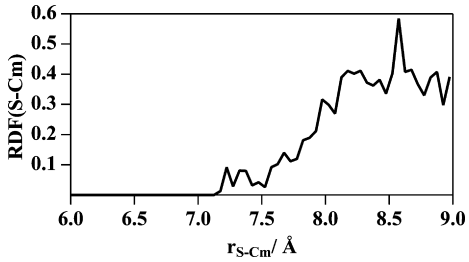

Figure 6. SDS-CH_4 RDF of S from Cm obtained in presence of water molecules at 275 K and p = 8 MPa.

interact with water rather than between them. To investigate the role of SDS-H_2O and CH_4−H_2O interactions in the context of the SDS-CH_4-$(H_2O)_{2000}$ system, the RDFs of SDS-H_2O and CH_4−H_2O have been also analyzed. The SDS-H_2O RDF shows the expected behavior in agreement with data from literature.[51] Figure 7 reports the S-Ow and S-Hw radial distribution

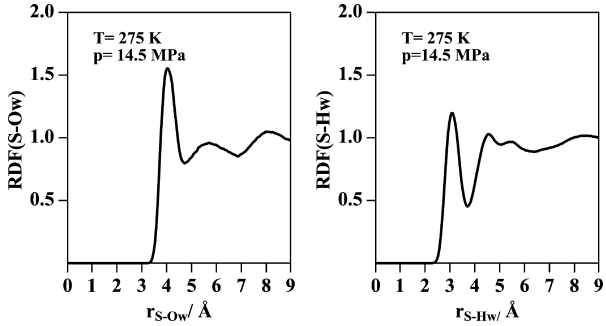

Figure 7. SDS-H_2O RDF of S from Ow and Hw at 275 K and p = 14.5 MPa.

functions evaluated at the conditions indicated in the figure. Very similar RDFs have been observed again at different conditions of p and T. The RDFs corresponding to CH_4-H_2O are presented in Figure 8. At the lower pressure investigated, the Cm-Ow radial distribution functions show a near-neighbor peak for r_{Cm-Ow} located at 3.725 and 3.625 Å at 275 and 291 K,

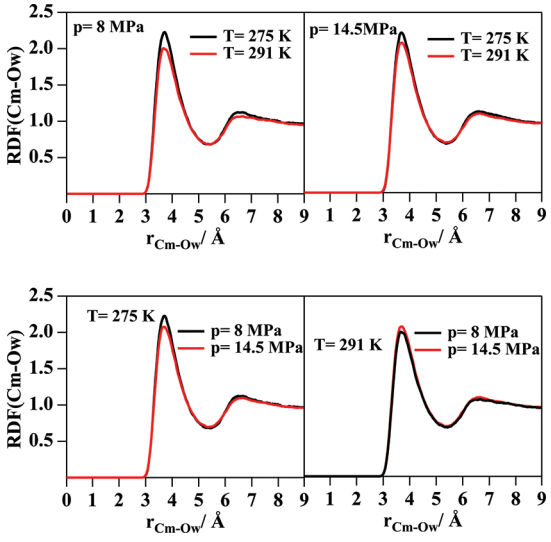

Figure 8. CH_4-H_2O RDF of Cm from Ow obtained at the different conditions indicated in the various panels.

dx.doi.org/10.1021/jp301124z | J. Phys. Chem. B 2012, 116, 4220−4227

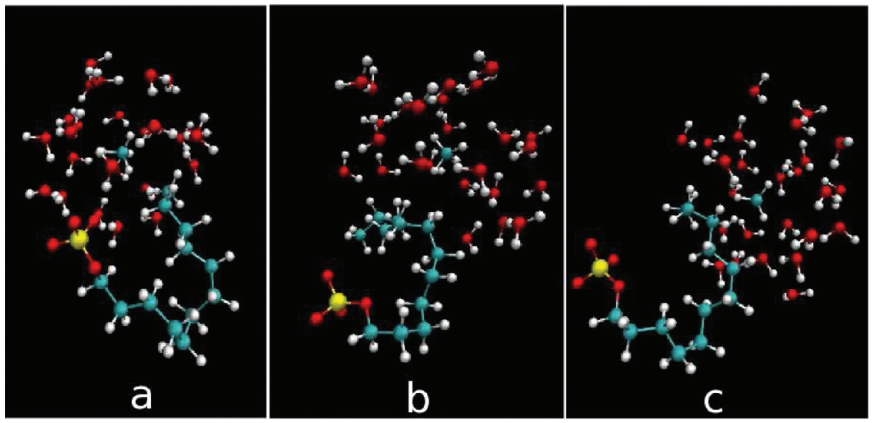

Figure 9. Consecutive screen shots of the clathrate formation mechanism for the solvated SDS-CH_4 system.

respectively. These results are similar to those reported in the literature though obtained under different conditions[54,55] and confirm that, in agreement with previous expectations,[52] only small changes are promoted by variation of p and T. Moreover, recent theoretical studies of host−guest interaction in gas hydrates,[56] considering only one methane molecule in a dodecahedral water cage found the shortest Cm-Ow distance equal to 3.720 Å. This confirms that, as already mentioned, clear modifications of the RDFs functions can be observed only when hydrate clathrate is completely formed and when more than one methane molecule is used.

Despite that, additional information, obtained by analyzing the positions of the nearest molecules of water around methane while integrating the trajectories of the SDS-$CH_4(H_2O)_{2000}$ system, allowed us to single out in a pictorial fashion the peculiar dynamical features of the methane clathration process (see the sequence of the *a*, *b* and *c* screen shots of Figure 9, obtained from simulations performed at 275 K and a pressure of 8 MPa). The sequence tells us that:

(a) An appropriate additive (such as a single SDS molecule) is sufficient to catalyze the process.
(b) The catalytic effect is due to the folding of SDS that drives water molecules to form a cage suitable to host a CH_4 molecule.

As is apparent from the figure, in fact, when solvated the SDS-CH_4 dimer folds to drive water to form a kind of half cage in which the CH_4 (slipping out of its head position near the sulfate in the pure SDS-CH_4 configuration illustrated Figure 2) ends up basketed (see panel a of Figure 9) in the created half cage. The arrangement of such partial 5^{12} cage is illustrated in detail in Figure 10 in which half of the 12 pentagons (for a total of 18 molecules) forming the whole clathrate structure are evidenced. Subsequently, the SDS molecule moves away (see b and c panels of Figure 9) allowing the completion of the clathrate cage formation and becoming available for a possible replication of the process.

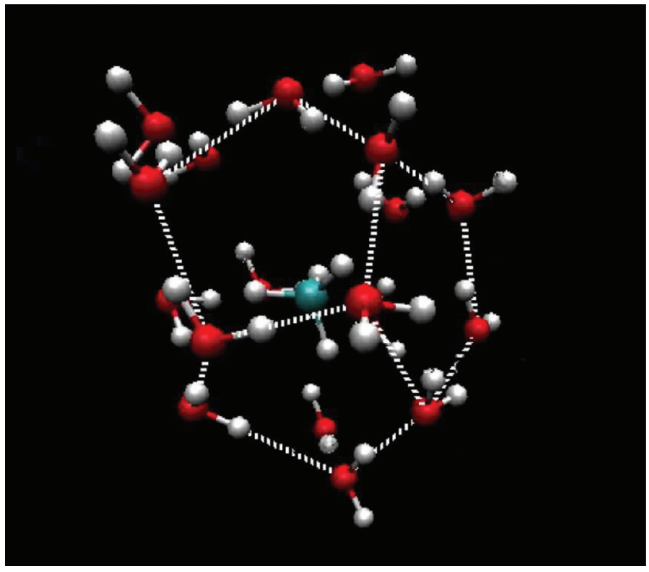

Figure 10. Sketch of the solvation sphere of methane at the end of the simulation. From the figure half of the structure 5^{12} of clathrates can be identified.

5. CONCLUSIONS

By exploiting the advantage of using a PES based on an improved formulation of intra- and intermolecular interaction utilizing the decomposition of the molecular polarizability, we have carried out a molecular dynamics investigation to the end of putting on a solid theoretical ground the mechanism proposed for the formation of methane clathrate hydrates. In particular we have investigated how the SDS exploits its catalytic effect in the formation of methane clathrate hydrate. The MD simulations were performed, first, for NVE ensembles of SDS-H_2O and SDS-CH_4 molecular components of the system and of their solvated forms in water. Then, NpT calculations for a system containing one molecule of surfactant and one molecule of gas but 2000 water molecules of the solvent were performed. In particular, the behavior of an SDS-CH_4 system surrounded by 2000 water molecules was followed in detail to the end of rationalizing the role played by SDS in catalyzing the formation of methane hydrate. The simulation singled out that the folding of the SDS in water solutions is the crucial dynamical step to create an incipient 5^{12} structure able to capture methane as a clathrate even when SDS micelles cannot be form confirming so far the experimental indications of a previous work.[15]

Moreover, the MD simulations agree with he rationalization of previous experiments carried out in a completely different context by Soper et al.[52] which shed some light on the way the solvation sphere modifies when clathrates are formed.

dx.doi.org/10.1021/jp301124z | J. Phys. Chem. B 2012, 116, 4220−4227

AUTHOR INFORMATION

Corresponding Author

*E-mail: m.alberti@ub.edu.

Notes

The authors declare no competing financial interest.

ACKNOWLEDGMENTS

M. Albertí acknowledges financial support from the Ministerio de Educación y Ciencia (Spain, Projects CTQ2010-16709 and PR2010-0243) and to the Comissionat per a Universitats i Recerca del DIUE (Generalitat de Catalunya, Project 2009-SGR 17). Also thanks are due to the Centre de Serveis Científics i Acadèmics de Catalunya CESCA and Fundació Catalana per a la Recerca for the allocated supercomputing time and to the COMPCHEM virtual organization of EG1 for access to the grid infrastructure. A. Costantini acknowledges financial support from Regione Umbria (POR UMBRIA FSE 2007-2013). A. Laganà, A. Costantini, and F. Pirani acknowledge financial support from the COST Action CM1002 (CODECS), INSTM, and the Italian Ministry of University and Research (MIUR) for a PRIN Grant. The authors wish to thank Prof. G. Savelli and his collaborators for stimulating discussions.

REFERENCES

(1) Kvenvolden, K. A. *Rev. Geophys.* **1993**, *31*, 173.
(2) Hammerschmidt, E. G. *Ind. Eng. Chem.* **1934**, *26*, 851.
(3) Chatti, I.; Delahaye, A; Fournaison, L.; Petitet, J. P. *Ener. Conv. Mang.* **2005**, *46*, 1333.
(4) Sloan, E. D., Jr. *Nature* **2003**, *426*, 353.
(5) Vatamanu, J.; Kusalik, P. G. *J. Phys. Chem. B* **2008**, *112*, 2399.
(6) Koh, C. A.; Sloan, D. *AIChE* **2007**, *53*, 1636.
(7) Alavi, S.; Woo, T. K. *J. Chem. Phys.* **2007**, *126*, 044703.
(8) Zhang, J. S.; Lo, C.; Somasundaran, P.; Lu, A.; Couzis, A.; Lee, J. W. *J. Phys. Chem. C* **2008**, *112*, 12381.
(9) Okano, Y.; Yasuoka, K. *J. Chem. Phys.* **2006**, *124*, 024510.
(10) Vysniauskas, A.; Bishnoi, P. R. *Chem. Eng. Sci.* **1983**, *38*, 1061.
(11) Sloan, E. D., Jr. *Clathrate Hydrates of Natural Gases*, 3rd ed.; CRC Press: Boca Raton, FL, 2008.
(12) Jiang, G.; Yunzhong, T.; Ning, F.; Zhang, L.; Dou, B.; Wu, X. *Proceedings of the 6th International Conference on Gas Hydrates (ICGH 2008)*, Vancouver, British Coulumbia, 2008.
(13) Zhang, J. S.; Lee., S.; Lee, J. W. *Ind. Eng. Chem. Res.* **2007**, *46*, 6353.
(14) Zhong, Y.; Rogers, R. E. *Chem. Eng. Sci.* **2000**, *55*, 4175.
(15) Di Profio, P.; Arca, S.; Gerani, R.; Savelli, G. *Chem. Eng. Sci.* **2005**, *60*, 4141.
(16) Costantini, A.; Laganà, A.; Pirani, F.; Maris, A.; Caminati, W. *Lecture Notes in Computer Science* **2005**, *3480*, 1046.
(17) Costantini, A.; Laganà, A.; Pirani, F. *Lecture Notes in Computer Science* **2006**, *3980*, 738.
(18) Costantini, A.; Laganà, A. *Lecture Notes in Computer Science* **2008**, *5072*, 1052.
(19) Costantini, A.; Albertí, M.; Pirani, F.; Laganà, A. *Int. J. Quantum Chem.* **2012**, *112*, 1810.
(20) Pirani, F.; Albertí, M.; Castro, A.; Moix, M.; Cappelletti, D. *Chem. Phys. Lett.* **2004**, *394*, 37.
(21) Albertí, M.; Castro, A.; Laganà, A.; Pirani, F.; Porrini, M.; Cappelletti, D. *Chem. Phys. Lett.* **2004**, *392*, 514.
(22) Albertí, M.; Castro, A.; Laganà, A.; Moix, M.; Pirani, F.; Cappelletti, D.; Liuti, G. *J. Phys. Chem. A* **2005**, *109*, 2906.
(23) Albertí, M.; Aguilar, A.; Lucas, J. M.; Cappelletti, D.; Laganà, A.; Pirani, F. *Chem. Phys.* **2006**, *328*, 221.
(24) Albertí, M.; Pacifici, L.; Laganà, A.; Aguilar, A. *Chem. Phys.* **2006**, *327*, 105.
(25) Albertí, M.; Aguilar, A.; Lucas, J. M.; Pirani, F. *J. Phys. Chem. A* **2010**, *114*, 11964.
(26) Huarte-Larragaña, F.; Aguilar, A.; Lucas, J. M.; Albertí, M. *J. Phys. Chem. A* **2007**, *111*, 8072.
(27) Albertí, M.; Aguilar, A.; Lucas, J. M.; Cappelletti, D.; Laganà, A.; Pirani, F. *Chem. Phys.* **2006**, *328*, 221.
(28) http://www.cse.scitech.ac.uk/ccg/software/DL_POLY/.
(29) Laganà, A.; Riganelli, A.; Gervasi, O. *Lecture Notes in Computer Science* **2006**, *3980*, 665, http://www.eu-egee.org/compchem
(30) Costantini, A.; Gervasi, O.; Manuali, C.; Faginas Lago, N.; Rampino, S.; Laganà, A. *J. Grid Comput.* **2010**, *8* (4), 571.
(31) Albertí, M.; Aguilar, A.; Lucas, J. M.; Laganà, A.; Pirani, F. *J. Phys. Chem. A* **2007**, *111*, 1780.
(32) Albertí, M. *J. Phys. Chem. A* **2010**, *114*, 2266.
(33) Albertí, M.; Aguilar, A.; Bartolomei, M.; Cappelletti, D.; Laganà, A.; Lucas, J. M.; Pirani, F. *Lecture Notes in Computer Science* **2008**, *5072*, 1026.
(34) Albertí, M.; Aguilar, A.; Cappelletti, D.; Laganà, A.; Pirani, F. *Int. J. Mass Spectrom.* **2009**, *280*, 50.
(35) Albertí, M.; Aguilar, A.; Bartolomei, M.; Cappelletti, D.; Laganà, A.; Lucas, J. M.; Pirani, F. *Phys. Scripta* **2008**, *78*, 058108.
(36) Faginas Lago, N.; Huarte-Larragaña, F.; Albertí, M. *Eur. Phys. J. D* **2009**, *55*, 75.
(37) Paolantoni, M.; Faginas Lago, N.; Albertí, M.; Laganà, A. *J. Phys. Chem. A* **2009**, *113*, 15100.
(38) Albertí, M.; Faginas Lago, N.; Laganà, A.; Pirani, F. *Phys. Chem. Chem. Phys.* **2011**, *13*, 8422.
(39) Albertí, M.; N. Faginas Lago, N.; Pirani, F. *Chem. Phys.* **2011**, DOI: 10.1016/j.chemphys.2011.08.009.
(40) Pirani, F.; Brizi, S.; Roncaratti, L. F.; Casavecchia, P.; Cappelletti, D.; Vecchiocattivi, F. *Phys. Chem. Chem. Phys.* **2008**, *10*, 5489.
(41) Pirani, F.; Cappelletti, D.; Liuti, G. *Chem. Phys. Lett.* **2001**, *350*, 286.
(42) Albertí, M.; Aguilar, A.; Pirani, F. doi:10.1016/j.chemphys.2011.07.030.
(43) Albertí, M.; Aguilar, A.; Pirani, F. *J. Phys. Chem. A* **2009**, *113*, 14741.
(44) Watson, J.; Baker, T. A.; Bell, S. P.; Gann, A.; Levine, M.; Losick, R. *Biología Molecular del gen.*; 5th ed.; Panamericana: 2008
(45) Bruce, C. D.; Berkowitz, M. L.; Perera, L.; Forbes, M. D. E. *J. Phys. Chem. B* **2002**, *106*, 3788.
(46) Akin-Ojo, O; Szalewicz, K. *J. Chem. Phys.* **2005**, *123*, 134311.
(47) http://ambermd.org/dbase.html.
(48) Schulz, F.; Hartke, B. *ChemPhysChem* **2002**, *3*, 98.
(49) Llanio-Trujillo, J. L.; Marques, J. M. C.; Pereira, F. B. *J. Phys. Chem. A* **2011**, *115*, 2130.
(50) Egelstaff, P. A. *An Introduction to the Liquid State*; Oxford University Press: New York, 1992.
(51) Schweighofer, K. J.; Essmann, U.; Berkowitz, M. *J. Phys. Chem. B* **1997**, *101*, 3793.
(52) Koh, C. A.; Wisbey, R. P.; Wu, X.; Westacott, R. E.; Soper, A. K. *J. Chem. Phys.* **2000**, *113*, 15.
(53) Thompson, H.; Soper, A. K.; Buchanan, P.; Aldiwan, N.; Creek, J. L.; Koh, C. A. *J. Chem. Phys.* **2006**, *124*, 164508.
(54) Chau, P. L.; Mancera, R. L. *Mol. Phys.* **1999**, *96*, 109.
(55) Guillot, B.; Guissani, Y. *J. Chem. Phys.* **1993**, *99*, 8075.
(56) Kumar, P.; Sathyamurthy, N. *J. Phys. Chem. A* **2011**, *115*, 14276.